Full Paper

N-(Indazolyl)benzamido Derivatives as CDK1 Inhibitors: Design, Synthesis, Biological Activity, and Molecular Docking Studies

Demetrio Raffa[1], Benedetta Maggio[1], Stella Cascioferro[1], Maria Valeria Raimondi[1], Giuseppe Daidone[1], Salvatore Plescia[1], Domenico Schillaci[1], Maria Grazia Cusimano[1], Lucina Titone[2], Claudia Colomba[2], and Manlio Tolomeo[2]

[1] Dipartimento di Chimica e Tecnologie Farmaceutiche, Università degli Studi di Palermo, Palermo, Italy.
[2] Dipartimento Malattie Infettive e Servizio AIDS, Policlinico Universitario Paolo Giaccone, Palermo, Italy.

A series of *N*-1*H*-indazole-1-carboxamides has been synthesized and their effects on both CDK1 / cyclin B and the K-562 (human chronic myelogenus leukemia) cell line were evaluated. Using a computational model, we have observed that all the most active compounds **9e**, **f**, **i** – **n** exhibited the same binding mode of purvanalol A in the ATP-binding cleft. Although they were able to moderately inhibit the leukemic cell line K-562 and to show inhibitory activity against the Cdc2-Cyclin B kinase in the low micromolar range, they turned out to be non-cytotoxic against HuDe (IZSL) primary cell cultures from human derm. These preliminary results are quite encouraging in view of the low toxicity demonstrated by the above-mentioned compounds.

Keywords: Antiproliferative agents / CDK1 inhibitors / Docking / 1*H*-Indazole-3-carboxamides / *N*-(1*H*-Indazolyl)benzamides

Received: September 3, 2008; accepted: October 22, 2008

DOI 10.1002/ardp.200800159

Introduction

2,6,9-Substituted purine derivatives represent a class of potent and selective inhibitors of cyclin-dependent protein kinase (CDK) that have recently been found to be of potential use as anticancer drugs [1 – 3]. In particular, olomoucine **1** [4], roscovitine **2** [5], purvalanol A **3** [6], O^6-cyclohexylmethylguanine (NU2058) **4**, and its analoge NU61025 [7] are significant examples of such kind of molecules (Fig. 1).

They act by competing with ATP for binding in the CDK catalytic site located in a deep cleft between the two lobes of the protein kinase [8].

Four key features are essential for the interaction with CDKs, the presence of the flat hydrophobic purine ring and the opportune substitutions in the position 2, 6, and 9. The purine ring allows the interaction of the molecules with the hinge region, a flexible fragment consisting of 81 to 84 residues that connects the two lobes of the kinases [9]. In particular, ATP adenine moiety hydrogen-bonds the backbone oxygen of Glu81 and the backbone nitrogen of Leu 83, and these hydrogen bonds are typically emulated by the CDK inhibitors that bind to the hinge region; a third hydrogen bond to the backbone oxygen of Leu 83 has also been observed for olomoucine **1**, roscovitine **2**, purvalanol A **3**, and NU2058 **4** [9, 10].

As a part of our research, we synthesized some *N*-(heteroaryl)-2-iodobenzamides **6a** – **p** with the aim of ascertain their activity as fungicides (Scheme 1) [11, 12].

Among the synthesized benzamides, the *N*-(indazol-3-yl)benzamides **6o**, **p** have drawn our attention as potential CDK inhibitors because they contain the characteristic, common to the majority of CDK inhibitors, the capability to make hydrogen bonds with the molecular fork present in the hinge region of CDKs [9] (Fig. 2).

On the basis of the structures of known potent CDK inhibitors, we foresaw the following structural modifications on the *N*-(indazol-3-yl)benzamido skeleton: the

Correspondence: Prof. Demetrio Raffa, Dipartimento di Chimica e Tecnologie Farmaceutiche, Università degli Studi di Palermo, Via Archirafi, 32, I-90123-Palermo, Italy.
E-mail: demraffa@unipa.it
Fax: +39 91 623 6117

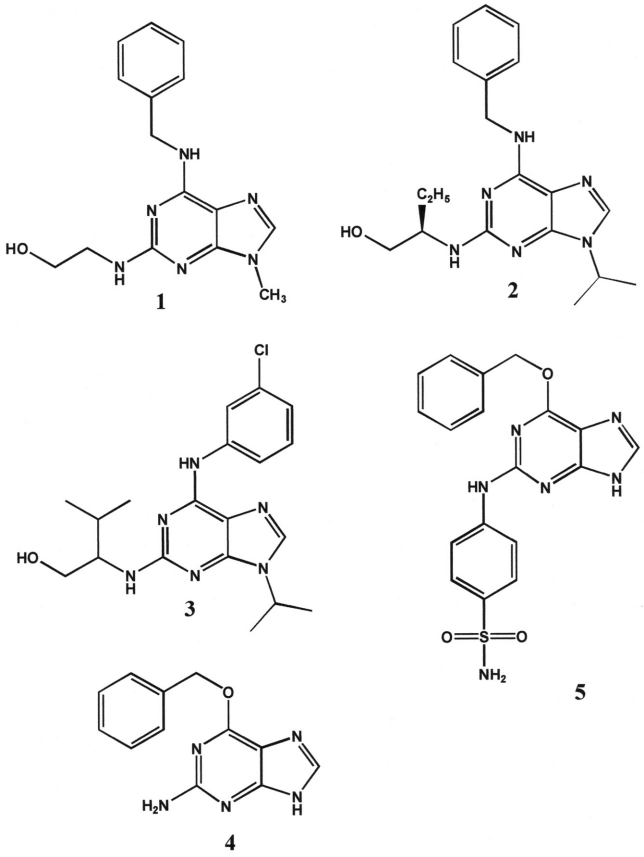

Figure 1. Chemical structures of some purine-derivative CDK inhibitors.

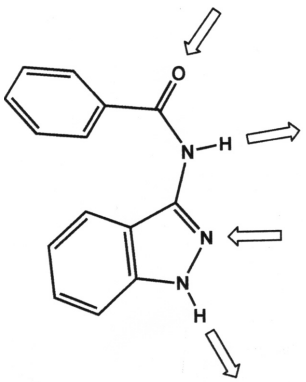

Figure 2. Potential hydrogen-bonding interactions of *N*-(indazol-3-yl)-benzamides with the hinge region.

introduction of various substituents on the benzamido moiety and its displacement from the 3-position of the indazole nucleus to the 5- and 6-positions, the amidic function inversion, and the substitution of the benzamido moiety with the phenoxyacetamido and phenylacetamido ones, with the goal to identify potent low molecular weight inhibitors of CDK1 that act by preventing the binding of the cofactor ATP to the enzyme. Molecular modelling and docking studies of the synthesized compounds were finally performed in order to rationalize the obtained CDK-inhibitory activities.

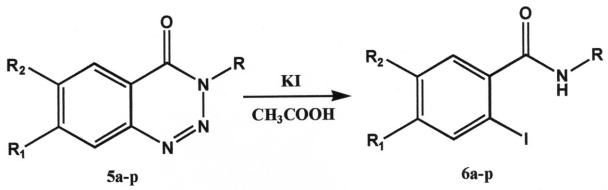

	R	R_1	R_2
a	3-methyl-isoxazol-5-yl	H	H
b	3-methyl-isoxazol-5-yl	Cl	H
c	3-methyl-isoxazol-5-yl	H	Cl
d	5-methyl-isoxazol-3-yl	H	H
e	5-methyl-isoxazol-3-yl	Cl	H
f	5-methyl-isoxazol-3-yl	H	Cl
g	1-phenyl-4carbetoxypyrazol-5-yl	H	H
h	1-phenyl-4carbetoxypyrazol-5-yl	Cl	H
i	1-phenyl-4carbetoxypyrazol-5-yl	H	Cl
l	Indazol-5-yl	H	H
m	Indazol-5-yl	Cl	H
n	Indazol-5-yl	H	Cl
o	Indazol-3-yl	Cl	H
p	Indazol-3-yl	H	Cl

Scheme 1. Synthetic pathway to obtain *N*-(heteroaryl)-2-iodobenzamides **6a**–**p**.

Results

Chemistry

The synthesis of *N*-(1*H*-indazol-3-yl)benzamides **9a** [12], **9b**–**f**, **9g** [13], **9h** [12], **9i** [12], **9l**–**n**, **9o** [14], 3,4-dichloro-*N*-(1*H*-indazol-5-yl)benzamide **11m** [13], 3,4-dichloro-*N*-(1*H*-indazol-6-yl)benzamide **13m**, *N*-(1*H*-indazol-3-yl)-2-phenoxyacetamide **16**, and *N*-(1*H*-indazol-3-yl)-2-phenylacetamide **17** [12] was obtained starting from commercially available benzoyl chloride precursors **7a**–**o**, **14**, **15**, and the opportune aminoindazole **8**, **10**, **12** as reported in Scheme 2.

The synthesis of the *N*-(3,4-dichlorophenyl)-1*H*-indazole-3-carboxamide **23** [15] and *N*-(5-chloro-2-iodophenyl)-1*H*-indazole-3-carboxamide **24** were carried out according to Scheme 3. The acylating agent diindazolo[2,3-*a*,2′,3′-*d*]pyrazine-7,14-dione **21** was obtained as follows: the 1*H*-indazole-3-carboxylic acid **18** was reacted with thionyl chloride as reported in the literature [16]. The 3,4-dichloroaniline **20** was purchased from Aldrich Chemical Company (Germany) and was used as received. The starting compound 5-chloro-2-iodoaniline **22** was obtained by reacting the 3-chloroaniline **19** with *N*-iodosuccinimmide (NIS) in acetic acid [17].

The structures of new compounds were characterized by analytical and spectroscopic measurements. The ^{1}H-NMR spectra of compounds **9**, **11**, **13**, **16**, **17** are consistent with the *N*-(1*H*-indazolyl)benzamido structure [18]. The

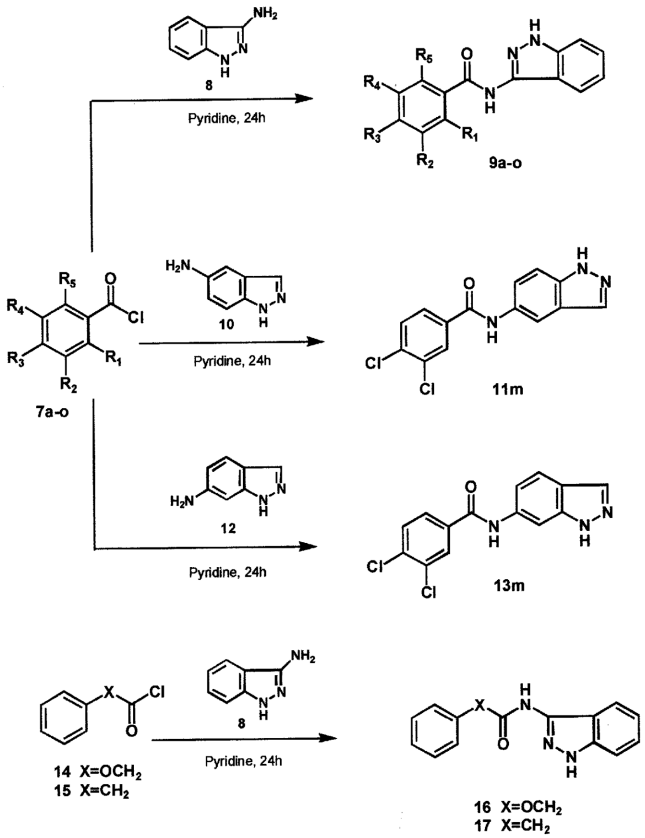

	a	b	c	d	e	f	g	h	i	l	m	n	o
R_1	H	I	Cl	H	H	H	H	H	H	H	H	F	NO_2
R_2	H	H	H	Cl	Br	F	OCH_3	H	H	H	Cl	H	H
R_3	H	H	H	H	H	H	H	Cl	F	I	Cl	H	H
R_4	H	H	H	H	H	H	H	H	H	H	H	H	Cl
R_5	H	H	H	H	H	H	H	H	H	H	H	F	H

Scheme 2. Synthetic pathway to obtain compounds **9a–o**, **11m**, **13m**, **16**, and **17**.

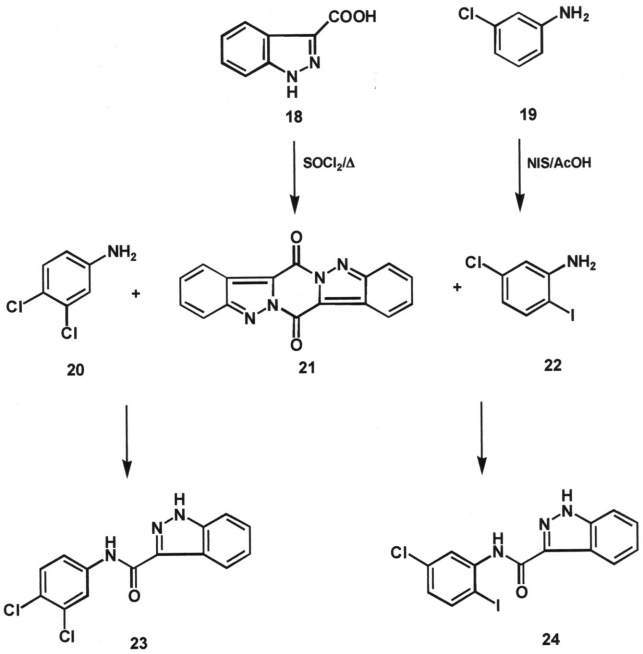

Scheme 3. Synthetic pathway to obtain compounds **23** and **24**.

aromatic protons appeared as multiplets at δ = 6.95 to 8.36 ppm, the benzamido NH protons appeared as singlets at δ = 10.49 to 11.14 ppm, while the indazole NH protons were found at δ = 12.68 to 13.04 ppm; compounds **16** and **17** also showed a singlet at δ = 4.82 ppm (OCH_2) and δ = 3.40 ppm (CH_2), respectively. The ^{1}H-NMR spectra of compounds **23** and **24** demonstrated a *N*-phenyl-1*H*-indazole-3-carboxamide structure [15]. The aromatic protons appeared as multiplets at δ = 7.29 to 8.36 ppm, the carboxamide NH protons appeared as singlets at δ = 10.69 to 10.71 ppm, while the indazole NH protons were found at δ = 13.86 to 13.88 ppm.

Molecular modelling methods

The crystallographic structure of CDK1 has not yet been determined, there is report of homology modelling of CDK1 [19]. The comparison between the sequences of the CDK1 and CDK2 proteins shows that these two proteins share 66% of identity with a similarity of 84%. Moreover, the sequence alignment and the contact shown that the binding sites of these two enzymes are very similar [19–21]. In particular, they present only two differences at positions 84 and 85 in their amino acidic composition which can be considered as minor difference, since their chains project outside the ATP-binding pocket and are not involved in ligand binding [20]. Furthermore, the hydrogen bond nucleoside recognition site remains relatively unchanged in the CDK1 model compared with the CDK2 crystal structure with a RMS (root mean square) deviation of the backbone on these residues of 0.23 Å [19]. Finally, the molecular fork identified in CDK2 structures seems to be conserved in the CDK1 structure suggesting that CDK1 may also be strongly inhibited by CDK2 inhibitors [21].

Based on these informations, the human thr160-phospho cdk2/cyclin A complexed with the inhibitor NU6102 **5**, which showed a resolution of 2.00 Å (Fig. 1; Brookhaven Protein Data Bank access code 1H1S) [22], was selected for the performance of molecular docking experiments

Insight II was used to check the 1H1S structure for missing atoms, bonds, and contacts. Cerius^2 4.10 was used to add hydrogens to the enzyme structure, to manually delete ligands and water molecules by saving only those that are able to form hydrogen bonds with the amino acids of the binding site (HOH5, HOH96, HOH120) [22].

Table 1. Percent inhibition of CDK1 at 10 μM concentration of **9a–o**, **11m**, **13m**, **16**, **17**, **23**, and **24**.

Comp.	**9a**	**9b**	**9c**	**9d**	**9e**	**9f**	**9g**	**9h**	**9i**	**9l**
	22.5	15.5	10.0	32.1	55.1	60.8	23.4	41.8	55.4	60.7
Comp.	**9m**	**9n**	**9o**	**11m**	**13m**	**16**	**17**	**23**	**24**	**PUR**
	60.3	49.9	16.9	ns	ns	10.0	ns	ns	ns	83.3

Values are the mean of at least three independent determinations; coefficient of variation was less than 15%; ns = not significant (%-inhibition <10%); PUR = purvanolol A.

The structure of NU6102 **5** (Fig. 1) was obtained with Cerius^2 4.10 by selecting and cutting the ligand from the protein-ligand complex.

Structures of the designed derivatives **9a–o**, **11m**, **13m**, **16**, **17**, **23**, and **24** were generated by molecular modelling with Cerius^2 4.10 software by optimizing their geometry using the Dreiding 2.21 force field with Gasteiger charges.

The active site of 1H1S was defined by the "docked ligand" procedure in the program Cerius^2 4.10 according to the shape of the ligand NU6102 **5** as grid points around this one which are unoccupied by protein atoms. A rigid docking experiment was performed for NU6102 **5** and, the ligand-fit predicted conformation of NU6102 **5** shows a high overlap with its x-ray crystallographic structure with a RMS of 1.02.

All inhibitors were docked into the active site of 1H1S to generate the docked conformations using the flexible docking procedure of "ligand fit" in the program Cerius^2 4.10.

Biology

CDK1 inhibitory activity

The CDK1 inhibitory activity for derivatives **9a–o**, **11m**, **13m**, **16**, **17**, **23**, and **24** was determined in-house in a non-radioisotopic assay (CycLex Cdc2-Cyclin B kinase assay kit) using purvanolol A as reference compound. The results as percent of CDK inhibition at 10 μM concentration are reported in Table 1. The IC_{50} values for compounds that exhibit at least 50% of CDK inhibition at screening concentration are reported in Table 2.

Tumour cell line screening

Synthesized *N*-(indazolyl)benzamido derivatives **9a–o**, **11m**, **13m**, **16**, **17**, **23**, and **24** were tested *in vitro* for their antileukemic activity against the K-562 (human chronic myelogenus leukemia) cell line. The results are reported in Table 3 as percent of growth inhibition at 10 μM concentration.

Table 2. IC_{50} values for compounds **9e**, **f**, **i–n** that exhibit at least 50% of CDK inhibition at screening concentration.

Compound	**9e**	**9f**	**9i**	**9l**	**9m**	**9n**	**PUR**
IC_{50} (μM)	6.6	4.4	8.8	9.8	6.0	10.0	1.8

Values are the mean of at least three independent determinations; coefficient of variation was less than 15%; PUR = purvanolol A.

Table 3. Percent-growth inhibition recorded on K562 cell line at 10 μM concentration of **9a–o**, **11m**, **13m**, **16**, **17**, **23**, and **24**.

Comp.	**9a**	**9b**	**9c**	**9d**	**9e**	**9f**	**9g**	**9h**	**9i**	**9l**
	35.9	ns	43.6	34.2	45.2	38.8	23.4	25.4	36.5	33.3
Comp.	**9m**	**9n**	**9o**	**11m**	**13m**	**16**	**17**	**23**	**24**	
	51.4	ns	39.7	ns	23.5	24.1	25.4	ns	29.1	

Values are the mean of at least three independent determinations; coefficient of variation was less than 15%; ns = not significant (%-inhibition <10%).

Table 4. IC_{50} values (μM) for compounds **9e**, **f**, **i–n** that exhibit at least 50% of inhibition on HuDe (IZSL), primary cell cultures from human derm.

Comp.	**9e**	**9f**	**9i**	**9l**	**9m**
	180	>200	>200	178	90

Values are the mean of at least three independent determinations; coefficient of variation was less than 15%; ns = not significant (% inhibition <10%).

Cytotoxicity for normal cells

To obtain more insights into the cytotoxic potential of tested compounds for normal human cells, the compounds **9e**, **f**, **i–n** were tested *in vitro* for their cytotoxicity against HuDe (IZSL), primary cell cultures from human derm (Table 4). All the tested compounds showed an IC_{50} greater than the cytotoxic activity on K-562.

Cell-cycle analysis

Because molecules exhibiting activity on CDK should cause the alteration of cell-cycle parameters, the effects of **9m** on cell-cycle distribution was analyzed in K562 cells. Cells were cultured for 24 h in the presence of **9m** used at the cytostatic concentration evaluated after 24 h of treatment (20 μM). Flow-cytometric analysis of the cell cycle was carried out as described in Experimental (Section 4.3.4) and reported in Fig. 3. The analysis of cell cycle of K562 cells exposed 24 h to **9m** showed a recruitment of cells in the late S-phase and in G2 / M. This is consistent with the ability of **9m** to inhibit CDK1 which is involved in the S-G2-M transition.

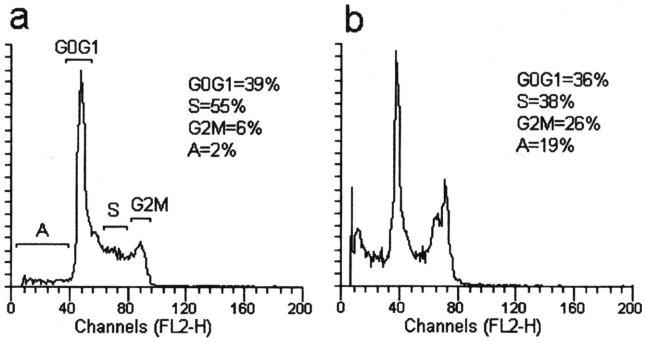

Figure 3. Effects of compound **9m** on DNA content / cell following treatment of K562 cells for 24 h. The cells were cultured without compound (control, panel a) or with **9m** used at a cytostatic concentration (panel b). Cell cycle distribution was analyzed by the standard propidium-iodide procedure as described in the Experimental Section. Sub-G0-G1 (A), G0-G1, S, and G2-M cells are indicated in panel a.

Discussion

An evaluation of the data reported in Table 1 revealed that the synthesized *N*-(indazolyl)benzamido derivatives **9a – o** are endowed with inhibitory activity against the CDK1 ranging from 10.0 to 60.8% at 10 μM concentration. As far as structure-activity relationships are concerned, it seems that the introduction of substituents in the positions 3 and 4 of the benzamido moiety (compounds **9d – m**) is favorable for the CDK1 inhibition with respect to the unsubstituted one **9a**, which is scarcely active (Table 1). Moreover, a decrease in inhibitory activity was demonstrated when the substituent in position 2 of the benzamido moiety (compounds **9b**, **c**) is exchanged. The displacement from the 3-position of the indazole nucleus to the 5- and 6-positions (compounds **11m** and **13m**), the substitution of the benzamido moiety with the phenoxyacetamido and phenylacetamido ones (compounds **16** and **17**), and the amidic function inversion (compounds **23** and **24**) gave rise to inactive or scarcely active compounds. To rationalize the SAR observed for *N*-(indazolyl)benzamido derivatives, compounds **9a – o**, **11m**, **13m**, **16**, **17**, **23**, and **24** were docked into the human thr160-phospho cdk2 / cyclin A (1H1S) together with the reference inhibitor purvanalol A. Comparison of the different docking results of the most active compounds **9e**, **f**, **i – n**, and purvanalol A **3** shows that, in principle, they adopt the same binding mode in the ATP-binding cleft (Fig. 4). The ligands are oriented so that their benzamido groups at C3 overlappes with the 3-chloroaniline group at N6 of purvanalol A. Furthermore, concerning the indazole nucleus, the pyrazole and phenyl rings overlapped with the imidazole ring and the N9 isopropyl side chain of purvanalol A, respectively. The

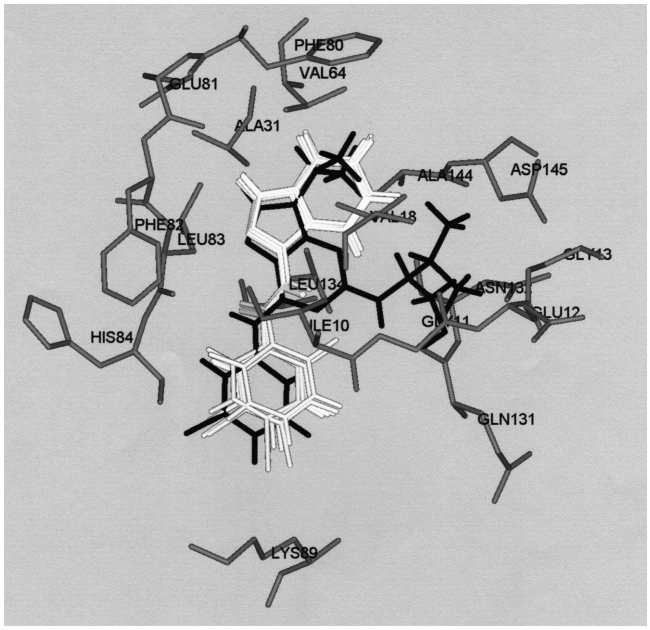

Figure 4. Overlay of the docked orientation for compounds **9e**, **f**, **i – n** (white) and purvanalol A (black) docked in the human thr160-phospho cdk2 / cyclin A (1H1S).

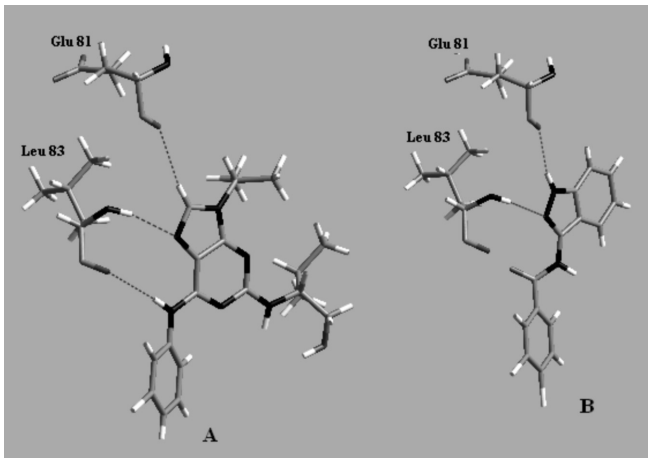

Figure 5. Purvanalol A (A) and compound **9m** (B) docked in the human thr160-phospho cdk2 / cyclin A (1H1S). Hydrogen bonds are indicated as dashed lines, nitrogens are in black, oxygens are in dark grey.

most important CDK2 / purvanalol A-simulated close contacts involve residues Ile10, Gly11, Gly13, Ala31, Val64, Phe80, Glu81, Phe82, Leu83, His84, Gln85, Asp86, Lys89, Asn132, Leu134, Ala144, Asp145, HOH5, and HOH96 while, in a similar way, CDK2-actives-simulated close contacts involve residue Ile10, Gly11, Val18, Ala31, Val64, Phe80, Glu81, Phe82, Leu83, His84, Gln85, Leu134, HOH5, and HOH96.

As can be seen in Fig.5, according to literature data [6], purvanalol A forms a complete triplet of hydrogen bonds

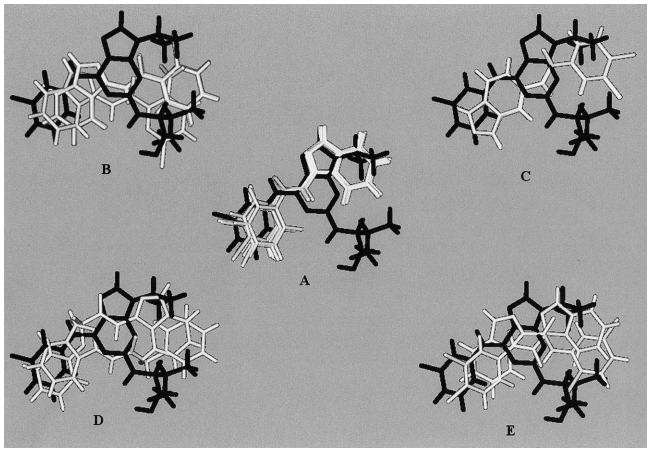

Figure 6. Overlay of the docked orientation for purvanalol A (black) and (A) active compounds **9e**, **f**, **i**–**n**, or inactive: (B) compounds **9b**, **c**, **o**; (C) compounds **11m**, **13m**; (D) compounds **16**, **17**; (E) compounds **23**, **24**.

between the N7-imidazole nitrogen and the backbone nitrogen of Leu83 (distance = 2.20 Å), the N6-amino group and the backbone oxygen of Leu83 (distance = 2.42 Å), and the acidic C8 atom of the purine ring and the backbone oxygen of Glu81 (distance = 2.72 Å). Compound **9m**, forms only a pair of bidentate hydrogen bonds between the N2-indazole nitrogen and the backbone nitrogen of Leu83 (distance = 2.17 Å) and N1 indazole nitrogen and the backbone oxygen of Glu81 (distance = 2.45 Å); the same intermolecular hydrogen bonds of **9m** were observed for all the other most active *N*-(indazolyl)benzamides **9e**, **f**, **i**, **l**, **n**.

The unsubstituted derivative **9a** showed a moderate inhibitory activity against the CDK1 (22.5% at screening concentration of 10 μM), even adopting the same binding mode of the most active compounds **9c**, **f**, **i**–**n** in the ATP-binding cleft. A comparison of the Connolly surfaces of **9a**, purvanalol A and the most active compounds **9c**, **f**, **i**–**n** showed that the presence of the substituents in the positions 3 and 4 determines an increase of the surface in this region with respect to the unsubstituted **9a** and, consequently, a greater number of positive hydrophobic interactions with Lys89, Asp86, and Gln85.

Moreover, inactive (**11m**, **13m**, **17**, **23**, **24**) and scarcely active (**9a**, **b**, **c**, **g**, **n**, **o**, **16**) compounds adopt a binding mode different from purvanalol A (Fig. 6) and form one or no hydrogen bonds with the hinge region.

These results are in agreement with the inhibitory activity against CDK1 reported for purvanalol A **3** and *N*-(indazolyl)benzamides (Tables 1 and 2).

The *in-vitro* testing for compounds **9a-o**, **11m**, **13m**, **14**, **15**, **21**, and **22** (Table 3) indicated that the *N*-(indazolyl)-benzamido derivatives are endowed with antiproliferative activity against the leukemic cell line K-562 (human chronic myelogenus leukemia). Comparison between the CDK1 inhibitory activity and the antiproliferative activity against K-562 showed a correlation between the two series of data; compounds that exhibited the higher CDK inhibition (**9e**, **f**, **i**–**n**) are, in principle, also endowed with an antiproliferative activity against K-562 ranging from 33.3 to 51.4% at 10 μM concentration. Finally, although the compounds **9e**, **f**, **i**–**n** were able to moderately inhibit the leukemic cell line K-562 and to show inhibitory activity against the Cdc2-Cyclin B kinase in the low micromolar range, they show a very low cytotoxicity against HuDe (IZSL), primary cell cultures from human derm, and these preliminary results are quite encouraging in view of the low toxicity shown by the above-mentioned compounds. Further investigation of the structure-activity and toxicity of this kind of compounds are currently underway in our group, and results will be published elsewhere.

Financial support from MIUR (PRIN 2006) is gratefully acknowledged.

Experimental

Chemistry

Reaction progress was monitored by TLC on silica gel plates (Merck 60, F_{254}, 0.2 mm; Merck, Germany). Organic solutions were dried over Na_2SO_4. Evaporation refers to removal of solvent on a rotary evaporator under reduced pressure. All melting points were determined on a Büchi 530 capillary melting point apparatus and are uncorrected (Büchi Labortechnik, Flawil, Switzerland). IR spectra were recorded with a Perkin Elmer Spectrum RXI FT-IR System spectrophotometer (Perkin-Elmer, Norwalk, CT, USA) as solid in KBr disc or nujol mull supported on NaCl disks. ^{1}H-NMR spectra were obtained using a Bruker AC-E 250-MHz spectrometer (Bruker Bioscience, USA) tetramethylsilane as an internal standard): chemical shifts are expressed in δ values (ppm). Mass spectra to 70 eV were obtained using an Autospec Ultima Ortogonal T.O.F.T. (Micromass, Manchester, UK) spectrometer or a GC-MS Varian Star 3400cx Saturn III spectrometer (Varian Inc., Palo Alto, CA, USA). Merck silica gel (Kiesegel 60/230–400 mesh) was used for flash chromatography columns. Microanalyses (C, H, N) performed in the laboratories of the Dipartimento di Scienze Farmaceutiche, Università degli Studi di Catania, are within ± 0.4% of the theoretical values. Yields refer to purified products and are not optimized.

*General procedure for the preparation of compounds **9**, **11**, **13**, **16**, and **17***

To a cold (ice bath 0–5°C) magnetic stirred solution of the opportune aminoindazole **8**, **10**, and **12** (4.3 mmol) in pyridine (5.37 mL), 4.3 mmol of the proper benzoyl chloride **7a**–**o**, **14**, **15** was added dropwise. The reaction mixture was left under magnetic stirring overnight and was then poured in crushed ice. The

solid, which separated, was filtered off and crystallized to give pure **9a – o**, **11m**, **13m**, **16**, and **17**.

N-(1H-Indazol-3-yl)-2-iodobenzamide ***9b***

Yield: 41%; m.p.: 180 – 182°C (ethyl acetate / chloroform); IR (KBr) ν [cm^{-1}]: 3275 (NH), 1658 (CO); ^{1}H-NMR (DMSO-d_6) δ [ppm]: 7.07 – 7.97 (a set of signals, 8H, aromatic protons), 10.82 (s, 1H, NH, exchangeable), 12.77 (s, 1H, NH, exchangeable). Anal. ($C_{14}H_{10}IN_3O$) C, H, N.

2-Chloro-N-(1H-indazol-3-yl)benzamide ***9c***

Yield: 98%; m.p.: 139 – 140°C (ethyl acetate / chloroform); IR (KBr) ν [cm^{-1}]: 3232 (NH), 1657 (CO); ^{1}H-NMR (DMSO-d_6) δ [ppm]: 7.08 – 7.86 (a set of signals, 8H, aromatic protons), 10.84 (s, 1H, NH, exchangeable), 12.77 (s, 1H, NH, exchangeable). Anal. ($C_{14}H_{10}ClN_3O$) C, H, N.

3-Chloro-N-(1H-indazol-3-yl)benzamide ***9d***

Yield: 32%; m.p.: 165 – 168°C (ethyl acetate / chloroform); IR (KBr) ν [cm^{-1}]: 3249 (NH), 1645 (CO); ^{1}H-NMR (DMSO-d_6) δ [ppm]: 7.06 – 8.14 (a set of signals, 8H, aromatic protons), 10.93 (s, 1H, NH, exchangeable), 12.84 (s, 1H, NH, exchangeable). Anal. ($C_{14}H_{10}ClN_3O$) C, H, N.

3-Bromo-N-(1H-indazol-3-yl)benzamide 1-carboxamide ***9e***

Yield: 67%; m.p.: 172 – 175°C (ethyl acetate / chloroform); IR (KBr) ν [cm^{-1}]: 3225 (NH), 1644 (CO); ^{1}H-NMR (DMSO-d_6) δ [ppm]: 7.09 – 8.27 (a set of signals, 8H, aromatic protons), 10.93 (s, 1H, NH, exchangeable), 12.84 (s, 1H, NH, exchangeable). Anal. ($C_{14}H_{10}BrN_3O$) C, H, N.

3-Fluoro-N-(1H-indazol-3-yl)benzamide ***9f***

Yield: 67%; m.p.: 150 – 152°C (petroleum ether / chloroform); IR (KBr) ν [cm^{-1}]: 3196 (NH), 1637 (CO); ^{1}H-NMR (DMSO-d_6) δ [ppm]: 7.07 – 7.96 (a set of signals, 8H, aromatic protons), 10.87 (s, 1H, NH, exchangeable), 12.82 (s, 1H, NH, exchangeable). Anal. ($C_{14}H_{10}FN_3O$) C, H, N.

N-(1H-Indazol-3-yl)-3-methoxybenzamide ***9g***

Yield: 98%; m.p.: 205 – 207°C (ethyl acetate / chloroform); IR (KBr) ν [cm^{-1}]: 3282 (NH), 1651 (CO); ^{1}H-NMR (DMSO-d_6) δ [ppm]: 3.85 (s, 3H, OCH_3); 7.06 – 7.74 (a set of signals, 8H, aromatic protons), 10.75 (s, 1H, NH, exchangeable), 12.78 (s, 1H, NH, exchangeable). Anal. ($C_{15}H_{13}N_3O_2$) C, H, N.

4-Chloro-N-(1H-indazol-3-yl)benzamide ***9h***

Yield: 72%; m.p.: 208 – 210°C (ethyl acetate / chloroform); IR (KBr) ν [cm^{-1}]: 3264 (NH), 1661, 1646 (CO); ^{1}H-NMR (DMSO-d_6) δ [ppm]: 7.09 – 8.14 (a set of signals, 8H, aromatic protons), 10.88 (s, 1H, NH, exchangeable), 12.82 (s, 1H, NH, exchangeable). Anal. ($C_{14}H_{10}ClN_3O$) C, H, N.

4-Fluoro-N-(1H-indazol-3-yl)benzamide ***9i***

Yield: 86%; m.p.: 198 – 199°C (ethyl acetate); IR (KBr) ν [cm^{-1}]: 3218 (NH), 1646 (CO); ^{1}H-NMR (DMSO-d_6) δ [ppm]: 7.07 – 8.22 (a set of signals, 8H, aromatic protons), 10.83 (s, 1H, NH, exchangeable), 12.82 (s, 1H, NH, exchangeable). Anal. ($C_{14}H_{10}FN_3O$) C, H, N.

N-(1H-Indazol-3-yl)-4-iodobenzamide ***9l***

Yield: 42%; m.p.: 218 – 220°C (ethanol); IR (KBr) ν [cm^{-1}]: 3256 (NH), 1647 (CO); ^{1}H-NMR (DMSO-d_6) δ [ppm]: 7.06 – 7.95 (a set of signals, 8H, aromatic protons), 10.83 (s, 1H, NH, exchangeable), 12.79 (s, 1H, NH, exchangeable). Anal. ($C_{14}H_{10}IN_3O$) C, H, N.

3,4-Dichloro-N-(1H-indazol-3-yl)benzamide ***9m***

Yield: 86%; m.p.: 248 – 250°C (ethyl acetate / chloroform); IR (KBr) ν [cm^{-1}]: 3402, 3241 (NH), 1673 (CO); ^{1}H-NMR (DMSO-d_6) δ [ppm]: 7.10 – 8.36 (a set of signals, 7H, aromatic protons), 11.00 (s, 1H, NH, exchangeable), 12.86 (s, 1H, NH, exchangeable). Anal. ($C_{14}H_9Cl_2N_3O$) C, H, N.

2,6-Difluoro-N-(1H-indazol-3-yl)benzamide ***9n***

Yield: 56%; m.p.: 190 – 193°C (ethyl acetate / chloroform); IR (KBr) ν [cm^{-1}]: 3245 (NH, NH_2), 1677 (CO); ^{1}H-NMR (DMSO-d_6) δ [ppm]: 7.10 – 7.81 (a set of signals, 7H, aromatic protons), 11.14 (s, 1H, NH, exchangeable), 12.82 (s, 1H, NH, exchangeable). Anal. ($C_{14}H_9F_2N_3O$) C, H, N.

3,4-Dichloro-N-(1H-indazol-5-yl)benzamide ***11m***

Yield: 65%; m.p.: 270 – 272°C (ethanol); IR (KBr) ν [cm^{-1}]: 3266, 3153 (NH), 1634 (CO); ^{1}H-NMR (DMSO-d_6) δ [ppm]: 7.54 – 8.21 (a set of signals, 7H, aromatic protons), 10.40 (s, 1H, NH, exchangeable), 13.04 (s, 1H, NH, exchangeable). Anal. ($C_{14}H_9Cl_2N_3O$) C, H, N.

3,4-Dichloro-N-(1H-indazol-6-yl)benzamide ***13m***

Yield: 80%; m.p.: 270 – 272°C (ethanol); IR (KBr) ν [cm^{-1}]: 3327, 3166 (NH), 1649 (CO); ^{1}H-NMR (DMSO-d_6) δ [ppm]: 7.38 – 8.26 (a set of signals, 7H, aromatic protons), 10.49 (s, 1H, NH, exchangeable), 12.98 (s, 1H, NH, exchangeable). Anal. ($C_{14}H_9Cl_2N_3O$) C, H, N.

N-(1H-Indazol-3-yl)-2-phenoxyacetamide ***16***

Yield: 52%; m.p.: 158 – 160°C (ethyl acetate / chloroform); IR (KBr) ν [cm^{-1}]: 3358, 3201 (NH), 1678 (CO); ^{1}H-NMR (DMSO-d_6) δ [ppm]: 4.82 (s, 2H, OCH_2), 6.95 – 7.76 (a set of signals, 9H, aromatic protons), 10.50 (s, 1H, NH, exchangeable), 12.74 (s, 1H, NH, exchangeable). Anal. ($C_{15}H_{13}N_3O_2$) C, H, N.

N-(1H-indazol-3-yl)-2-phenylacetamide ***17***

Yield: 98%; m.p.: 229 – 230°C (chloroform); IR (KBr) ν [cm^{-1}]: 3282 (NH), 1669 (CO); ^{1}H-NMR (DMSO-d_6) δ [ppm]: 3.40 (s, 2H, CH_2), 7.02 – 7.74 (a set of signals, 9H, aromatic protons), 10.62 (s, 1H, NH, exchangeable), 12.68 (s, 1H, NH, exchangeable). Anal. ($C_{15}H_{13}N_3O$) C, H, N.

General procedure for the preparation of N-(3,4-dichlorophenyl)-1H-indazole-3-carboxamide ***23*** *and N-(5-chloro-2-iodophenyl)-1H-indazole-3-carboxamide* ***24***

A magnetically stirred solution of diindazolo[2,3-*a*, 2',3'-*d*]pyrazine-7,14-dione **21** [13] (2.37 mmol, 0.68 g) and the opportune aniline **20**, **22** (4.74 mmol, 1.2 g) in pyridine (13.5 mL), was left under magnetic stirring for seven days and then poured into crushed ice. The solid which separated was filtered off and crystallized to give the compounds **23** and **24**.

N-(3,4-Dichlorophenyl)-1H-indazole-3-carboxamide ***23***

Yield: 89%; m.p.: 266–268°C (petroleum ether / chloroform); IR (KBr) ν [cm^{-1}]: 3361, 3259 (NH), 1662 (CO); ^{1}H-NMR (DMSO-d_6) δ [ppm]: 7.31–8.36 (a set of signals, 7H, aromatic protons), 10.71 (s, 1H, NH, exchangeable), 13.88 (s, 1H, NH, exchangeable). Anal. ($C_{14}H_9Cl_2N_3O$) C, H, N.

N-(5-Chloro-2-iodophenyl)-1H-indazole-3-carboxamide ***24***

Yield: 23%; m.p.: 246–248°C (ethyl acetate); IR (KBr) ν[cm^{-1}]: 3254 (NH), 1663 (CO); ^{1}H-NMR (DMSO-d_6) δ [ppm] 7.29–8.30 (a set of signals, 7H, aromatic protons), 10.69 (s, 1H, NH, exchangeable), 13.86 (s, 1H, NH, exchangeable). Anal. ($C_{14}H_9ClIN_3O$) C, H, N.

Hardware and software

The docking experiments as well as receptor and ligand preparations were performed on a Silicon Graphics Fuel Visual Workstation (SGI, Sunnyvale, CA, USA), 1 GB memory with IRIX 64 release 6.5 operating system. The Insight II program 2005 (Accelrys Software Inc., San Diego, CA, USA) was used for receptor and structure manipulation and visualization of results. Cerius^2 4.10 program (Accelrys Software Inc., San Diego, CA, USA) was used for ligand construction and for molecular docking procedure.

Biology

CDK1 inhibition test

In order to estimate the inhibitory effect on individual Cdc2-Cyclin B activity in the test compounds, we have used a "Cdc2-Cyclin B Kinase Assay Kit" (cat#CY-1164, CycLex Co., Ltd). Plates are pre-coated with a substrate corresponding to recombinant Cdc7, which contains threonine residue that can be phosphorylated by Cdc2-Cyclin B but not Cdk2-Cyclin A, Cdk2-Cyclin E, Cdk4-Cyclin D, and Cdk6-Cyclin D *in vitro*. The detector antibody specifically detects only the phosphorylated form of threonine residue on Cdc7.

To perform the test, the sample is diluted in kinase buffer; 10 μL of inhibitor are pipetted into the wells with 80 μL kinase reaction buffer (kinase buffer / ATP 125 μM). To initiate reaction, Cdc2-Cyclin B (1.5m unit/μL) is added to each well at room temperature. Cdc2-Cyclin B positive control (90 μL of kinase reaction buffer with 10 μL of Cdc2-Cyclin B, without inhibitors) should be included in each assay as a positive control for phosphorylation. It is also necessary to conduct the control experiment of solvent control (80 μL of kinase reaction buffer, 10 μL of solvent for inhibitor and 10 μL of Cdc2-Cyclin B), inhibitor control (80 μL of kinase reaction buffer, 10 μL of 100 μM purvalanol A or an other known inhibitor and 10 μL of Cdc2-Cyclin B) and no-enzyme control (90 μL of kinase reaction buffer with 10 μL of buffer). Cover with plate sailer, and incubate at 30°C for 30 min. We have washed wells five times with wash buffer. The amount of phosphorylated substrate is measured by binding it with a 100 μL of solution of TK-3H7, an anti-phospho-Cdc7-Threonine376 antibody, followed by binding with 100 μL of solution of horseradish peroxidase conjugated anti-mouse IgG, which then catalyzed the conversion of the chromogenic substrate tetra-methylbenzidine (TMB) (100 μL of substrate reagent) from a colorless solution to a blue solution (or yellow after the addition of 100 μL of stopping reagent) (the washing with wash buffer at each step is essential for a good performance). The color is quantitated by spectrophotometry (at wavelength of 405 nm) and reflects the relative amount of Cdc2-Cyclin B activity in the sample.

In-vitro antiproliferative activity

Compounds **9a–o**, **11m**, **13m**, **16**, **17**, **23**, and **24** were tested *in vitro* for antiproliferative activity against K562 (human chronic myelogenous leukemia) cell line. These cell lines were grown at 37°C in a humidified atmosphere containing 5% CO_2, in RPMI-1640 medium supplemented with 10% fetal bovine serum and antibiotics.

K562 cells were suspended at a density of 1×10^5 cells/mL in growth medium, transferred to 24-well plate (1 mL/well), cultured with or without (in the case of control wells) a screening concentration of 10 μM of compounds and incubated at 37°C for 48 h. Numbers of viable cells were determined by counting in a hematocytometer after dye exclusion with trypan blue [23]. The antiproliferative effects of the compounds were estimated in terms of%-growth inhibition comparing cell viability of treated and untreated cells. We determined IC_{50} values (test agent concentration at which the cell proliferation was inhibited to 50% of the untreated growth control) for compounds that exhibited the best activity at the screening concentration.

Cytotoxicity for normal cells

We evaluated the cytotoxicity of compounds **9e**, **f**, **i–m** against HuDe (IZSL), primary cell cultures from human derm; such activity was determined by MTT (methylthiazotetrazolium) assay [24]. The cells were suspended at a density of 1×10^5 cells/mL in MEM (Sigma, USA), supplemented with 10% fetal calf serum and antibiotics, transferred (100 μL/well) to 96-well plate, and incubated at 37°C for three days until the formation of a cellular monolayer. After this time, the original medium was replaced with RPMI-1640 medium without red phenol (Sigma) and concentrations ranging from 100 to 1 μM of compounds were added to each well and incubated at 37°C for 24 h. The cytotoxic effects of the compounds were estimated in term of%-growth inhibition comparing cell viability of treated and untreated cells by their reduction of the tetrazolium substrate and IC_{50} values (test agent concentration at which the cell proliferation was inhibited to 50% of the untreated growth control) were determined.

Flow-cytometric analysis of cell-cycle distribution

The effects of compound **9m** on cell-cycle distribution were studied on K562 cells (myeloblastic leukemia) by flow-cytometric analysis after staining with propidium iodide. Cells were exposed 24 h to compound **9m**. After treatment, cells were washed once in ice-cold phosphate buffered saline medium (PBS; Sigma) and resuspended at 10^6/mL in a hypotonic fluorochrome solution of propidium iodide (Sigma, St Louis, MO, USA) (50 μg/mL) and nonidet P-40 (Sigma) [0.03% (v/v)] in 0.1% sodium citrate. After 30 min of incubation, the fluorescence of each sample was analyzed as single-parameter frequency histograms by using a FACScan flow cytometer (Becton Dickinson, San Jose, CA, USA). The distribution of cells in the cell cycle and the apoptotic subG0-G1 peak was analyzed with the ModFit LT3 program (Verity Software House, Inc., Topsham, ME, USA).

References

[1] D. Fabbro, S. Ruetz, E. Buchdunger, S. W. Cowan-Jacob, *et al.*, *Pharmacol. Ther.* **2002**, *93*, 79–98.

[2] P. L. Toogood, *Curr. Opin. Chem. Biol.* **2002**, *6*, 472–478.

[3] M. Knockaert, P. Greengard, L. Meijer, *Trends Pharmacol. Sci.* **2002**, *23*, 417 – 425.

[4] U. Schulze-Gahmen, J. Brandsen, H. D. Jones, D. O. Morgan, *et al.*, *Protein Struct. Funct. Genet.* **1995**, *22*, 378 – 391.

[5] W. F. de Azevedo, S. LeClerc, L. Meijer, L. Havlicek, *et al.*, *Eur. J. Biochem.* **1997**, *243*, 518 – 526.

[6] N. S. Gray, L. Wodicka, A. M. W. H. Thunnisen, T. C. Norman, *et al.*, *Science* **1998**, *281*, 533 – 538.

[7] C. E. Arris, F. T. Boyle, A. H. Calvert, N. J. Curtin, *et al.*, *J. Med. Chem.* **2000**, *43*, 2797 – 2804.

[8] P. D. Jeffrey, A. A. Russo, K. Polyak, E. Gibbs, *et al.*, *Nature* **1995**, *376*, 313 – 320.

[9] F. Candurri, W. F. de Azvedo Jr., *Current Computer-Aided Drug Design* **2005**, *1*, 53 – 64.

[10] T. G. Davies, D. J. Pratt, J. A. Endicott, L. N. Johnson, M. E. M. Noble, *Pharmacol. Ther.* **2002**, *93*, 125 – 133.

[11] D. Raffa, G. Daidone, B. Maggio, D. Schillaci, *et al.*, *Il Farmaco* **1999**, *54*, 90 – 94.

[12] D. Korbonits, I. Kanzel-Szvoboda, K. Horvath, *J. Chem. Soc. Perkin Trans. I* **1982**, *3*, 759 – 766.

[13] Compounds **9g** and **11m** are known (CAS numbers 883054-87-3 and 925634-33-9, respectively) but no references were found on SciFinder Scholar.

[14] D. Raffa, G. Daidone, F. Plescia, D. Schillaci, *et al.*, *Il Farmaco* **2002**, *57*, 183 – 187.

[15] F. K. Kirchner (Sterling Drug Inc. NY), US 3,457,269, **1969**; (Chem. Abstr. 1969, 71, P101851z).

[16] R. F. Smith, F. K. Kirchner, *J. Org. Chem.* **1958**, *23*, 621.

[17] J. Valgeirsson, E. O. Nielsen, D. Peters, C. Mathiesen, *et al.*, *J. Med. Chem.* **2004**, *47*, 6948 – 6957.

[18] G. Daidone, S. Plescia, D. Raffa, D. Schillaci, *et al.*, *Heterocycles* **1996**, *43(11)*, 2385 – 2396.

[19] C. F. McGrath, N. Pattabiraman, G. E. Kellog, T. Lemcke, *et al.*, *J. Biomol. Struct. Dyn.* **2005**, *22*, 493 – 502.

[20] P. Furet, J. Zimmermann, H. G. Capraro, T. Meyer, P. Imbach, *J. Computer-Aided Mol. Des.* **2000**, *14*, 403 – 409.

[21] F. Candurri, H. B. Uchoa, W. F. de Azevedo Jr., *Biochem. Biophys. Res. Comm.* **2004**, *324*, 661 – 666.

[22] T. G. Davies, J. Bentley, C. E. Arris, F. T. Boyle, *et al.*, *Nat. Struct. Biol* **2002**, *9*, 745 – 749.

[23] S. Manfredini, R. Bazzanini, P. G. Baraldi, M. Guarneri, *et al.*, *J. Med. Chem.* **1992**, *35*, 917 – 924.

[24] J. Carmicael, W. G. DeGraff, A. P. Gadzar, J. D. Minna, J. B. Mitchel, *Cancer Res.* **1987**, *47*, 936 – 942.

